Future temperature in southwest Asia projected to exceed a threshold for human adaptability

Jeremy S. Pal[1,2] and Elfatih A. B. Eltahir[2]★

A human body may be able to adapt to extremes of dry-bulb temperature (commonly referred to as simply temperature) through perspiration and associated evaporative cooling provided that the wet-bulb temperature (a combined measure of temperature and humidity or degree of 'mugginess') remains below a threshold of 35 °C. (ref. 1). This threshold defines a limit of survivability for a fit human under well-ventilated outdoor conditions and is lower for most people. We project using an ensemble of high-resolution regional climate model simulations that extremes of wet-bulb temperature in the region around the Arabian Gulf are likely to approach and exceed this critical threshold under the business-as-usual scenario of future greenhouse gas concentrations. Our results expose a specific regional hotspot where climate change, in the absence of significant mitigation, is likely to severely impact human habitability in the future.

The geologic formations beneath and around the Arabian Gulf (hereafter referred to as the Gulf) in Southwest Asia, commonly referred to as the Middle East, are a major source for the oil and gas consumed locally and around the world, contributing greatly to the past and current emissions of carbon dioxide[2]. Here, we show that by the end of the century certain population centres in the same region are likely to experience temperature levels that are intolerable to humans owing to the consequences of increasing concentrations of anthropogenic greenhouse gases (GHGs).

The 5th Assessment Report of the Intergovernmental Panel on Climate Change (IPCC) presents substantial evidence that increasing anthropogenic GHG concentrations are responsible for much of Earth's warming in recent decades[3]. Although observations and model simulations largely support this global climate change hypothesis, more research efforts are needed to improve understanding of impacts at regional and local scales. Some important limitations to the accuracy of global climate model (GCM) projections of these impacts stem from the lack of sufficient resolution needed to resolve regional processes and understand societal impacts; and the inadequate treatment of physical processes of regional importance[4,5]. To investigate dangers to human health of extreme heat and humidity in Southwest Asia, we apply a regional climate model (RCM) at a 25-km grid spacing specifically customized for the region[6–9] forced by three IPCC GCMs objectively selected based on performance (see Supplementary Methods). By conducting high-resolution RCM simulations, we resolve approximately 30 grid-points for each GCM grid-point, allowing a more detailed representation of topography, coastlines, extreme climatic events, and physical processes.

We consider both dry-bulb temperature (T) and wet-bulb temperature (TW), specifically their daily maxima averaged over 6 h, denoted by T_{max} and TW_{max}, respectively. Whereas the general public can easily relate to the concept of T, TW is not a widely used

and understood concept. It is the temperature an air parcel would attain if cooled at constant pressure by evaporating water within it until saturation[10]. It is a combined measure of temperature and humidity, or 'mugginess'.

Like all living species, human survival is partially a function of the environmental temperature. 35 °C is the threshold value of TW beyond which any exposure for more than six hours would probably be intolerable even for the fittest of humans, resulting in hyperthermia. In current climate, TW rarely exceeds 31 °C (ref. 1). Although other dry-bulb temperature and combined empirical temperature and humidity indices have been used to investigate the impacts of climate change on heat stress[11–15], TW provides a physically based relationship to the human body's core temperature.

For extreme temperature, we arbitrarily select 60 °C, a value close to the highest temperature ever reported on Earth[16,17]. In dry heat conditions, the human body is at high risk of heat stroke at temperatures well below 60 °C if not well hydrated and if exposed to the sun. In addition, when T approaches such extremes, much machinery designed for the current climate may malfunction. For example, aircraft may not operate properly during takeoff and landing, and rail lines can buckle at extreme temperatures, even at temperatures around 40 °C.

Under recent climate conditions (1976–2005) with historical GHG concentrations[18], the ensemble average of the largest TW_{max} event exceeds 31 °C, primarily in the Gulf and surrounding coastal regions (Fig. 1). These regions are located in low-elevation areas close to sea level allowing for high T, and near the coast allowing for high humidity. Interior desert regions have lower values of TW and TW_{max} owing to drier air. Although the 35 °C threshold is approached in many locations, it is not exceeded anywhere in the domain. In contrast, the ensemble average of the largest T_{max} events exhibits values exceeding 50 °C in some interior desert regions and in coastal areas, but relatively low values over the Gulf and Red Sea. These severe heat-related conditions located in relatively low areas located near water bodies are consistent with projected heat-wave conditions in southern Europe and Mediterranean coasts[13].

The high values of TW_{max} over the Red Sea and the Gulf are due to a combination of physical processes. First, the entire region experiences virtually clear sky conditions owing to subsidence during summer associated with the rising air motion over the monsoon region to the east[19]. The reason higher surface TW_{max} in this region fails to trigger deep convection is explained by persistent regional-scale subsidence, involving adiabatic and diabatic descent, which suppresses deep convection[19]. Subsidence over this region results in the absence of clouds and high incoming solar radiation. Second, unlike the surrounding deserts, the surface albedo of the Red Sea and the Gulf is relatively low, yielding strong absorption of solar radiation and increased total heat flux. Third, the high

[1]Department of Civil Engineering and Environmental Science, Loyola Marymount University, Los Angeles, California 90045, USA. [2]Ralph M. Parsons Laboratory, Massachusetts Institute of Technology, Cambridge, Massachusetts 02139, USA. *e-mail: eltahir@mit.edu
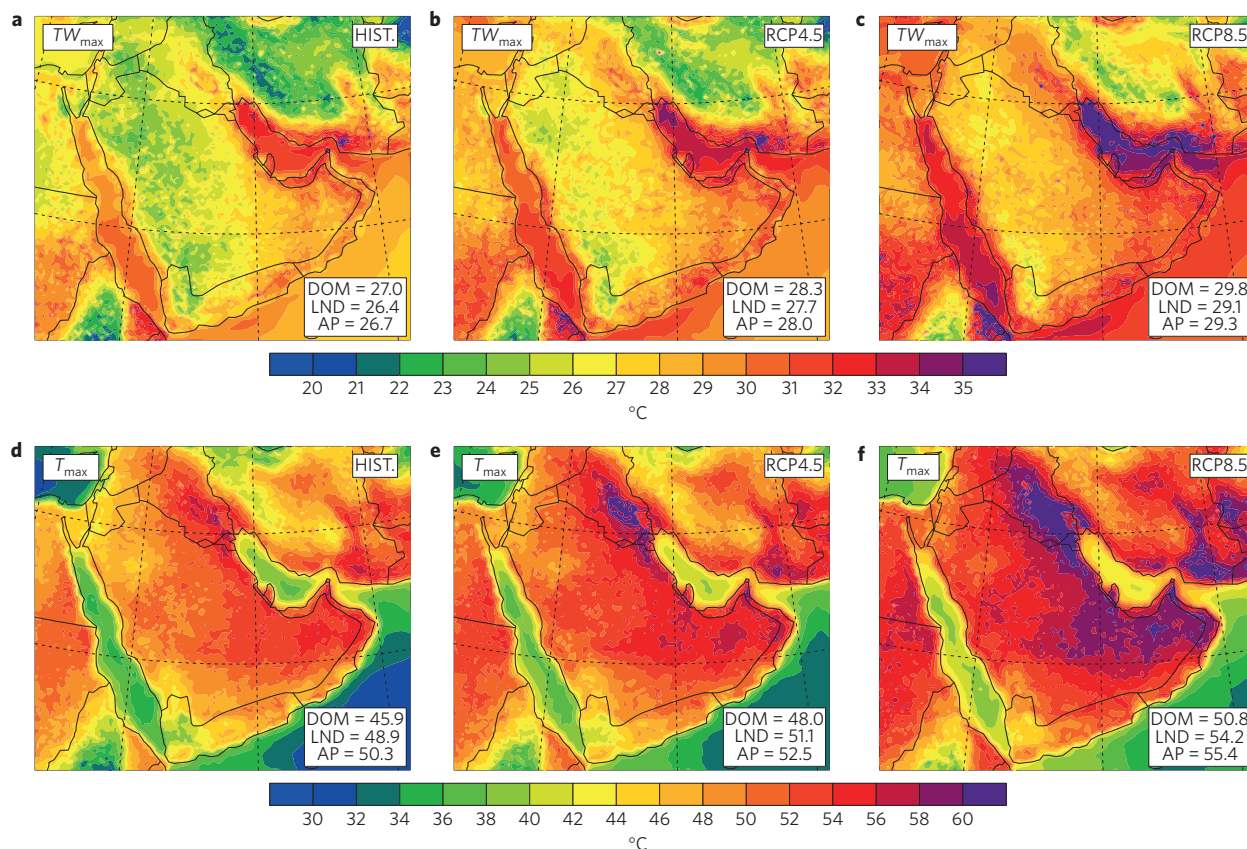
Figure 1 | Spatial distributions of extreme wet bulb temperature and extreme temperature. a–f, Ensemble average of the 30-year maximum TW_{max} (**a–c**) and T_{max} (**d–f**) temperatures for each GHG scenario: historical (**a,d**), RCP4.5 (**b,e**) and RCP8.5 (**c,f**). Averages for the domain excluding the buffer zone (DOM), land excluding the buffer zone (LND) and the Arabian Peninsula (AP) are indicated in each plot. TW_{max} and T_{max} are the maximum daily values averaged over a 6-h window.

evaporation rate increases water vapour and heat retained at the surface. The boundary layer is relatively shallow over these water bodies, concentrating water vapour and heat close to the surface. All these factors taken together maximize the total flux of heat into a relatively shallow boundary layer, hence maximizing the near-surface TW over these water bodies. Coastal locations surrounding these water bodies are thus susceptible to high TW via air transport (for example, sea breeze circulations).

To predict impacts of future climate change towards the end of the century (2071–2100), two GHG concentration scenarios are assumed, based on the IPCC Representative Concentration Pathway (RCP) trajectories: RCP4.5 (ref. 20) and RCP8.5 (ref. 21). RCP8.5 represents a business-as-usual scenario, whereas RCP4.5 considers mitigation. Under RCP8.5, the area characterized by TW_{max} exceeding 31 °C expands to include most of the Southwest Asian coastal regions adjacent to the Gulf, Red Sea and Arabian Sea (Fig. 1). Furthermore, several regions over the Gulf and surrounding coasts exceed the 35 °C threshold.

Annual TW_{max} increases monotonically in the different locations surrounding the Gulf (Fig. 2). By the end of the century, annual TW_{max} in Abu Dhabi, Dubai, Doha, Dhahran and Bandar Abbas exceeds 35 °C several times in the 30 years, and the present-day 95th percentile summer (July, August, and September; JAS) event becomes approximately a normal summer day (Fig. 3). During the summer, warm northwesterly (Shamal) winds frequently blow from Turkey and Iraq across the Gulf, where they gain moisture and transport high TW to most of the cities in the Gulf. The primary exceptions are Kuwait City and Bandar-e Mahshahr, which are protected from such extreme TW conditions owing to their geographic position to the north of the Gulf.

Extreme T_{max} events exceeding 45 °C become the norm in most low-lying cities during JAS (Supplementary Figs 8 and 9). Although being protected against extreme TW_{max} events, annual T_{max} is projected to exceed 60 °C in Kuwait City during some years. Annual T_{max} values exceeding 60 °C are also projected in Al Ain, which is somewhat isolated from the Gulf coast but still low in elevation. Doha is uniquely geographically positioned to receive hot dry air from the desert interior to the west and hot moist air from the Gulf. As a result, it is vulnerable both T and TW extremes.

On the coast of the Red Sea, milder conditions, but still fairly severe, are projected compared to the Gulf. In Jeddah and nearby Mecca, for example, annual TW_{max} is projected to reach values as high as 33 °C and 32 °C, respectively (Fig. 2), with annual T_{max} approaching and exceeding 55 °C (Figure SI8). These extreme conditions are of severe consequence to the Muslim rituals of Hajj, when Muslim pilgrims (~2 million) pray outdoors from dawn to dusk near Mecca. The exact date for this ritual is fixed according to the lunar calendar and can therefore occur during the boreal summer for several consecutive years. This necessary outdoor Muslim ritual is likely to become hazardous to human health, especially for the many elderly pilgrims, when the Hajj occurs during the boreal summer.

As the population in Southwest Asia continues to rapidly increase[22], cities will probably expand and new cities may emerge. The rise in annual T_{max} as a result of climate change would make the present harsh desert environments even harsher, while the rise in annual TW_{max} would probably constrain development along the coasts. The countries in Southwest Asia stand to gain considerable benefits by supporting the global mitigation efforts implied in the RCP4.5 scenario. Such efforts applied at the global scale would
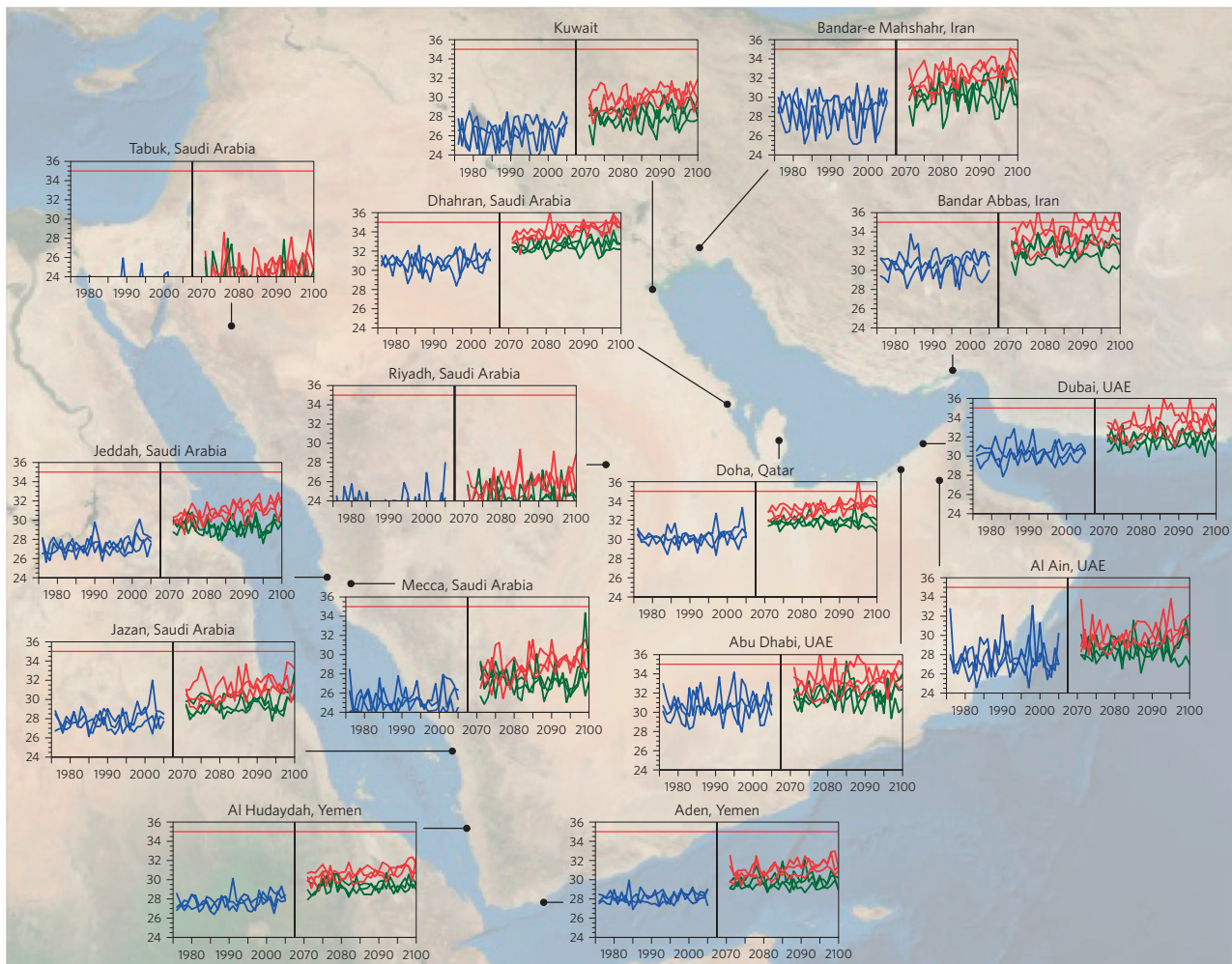
Figure 2 | Time series of the annual maximum TW_{max} for each ensemble member and GHG scenario. Blue, green and red lines represent the historical (1976–2005), RCP4.5 (2071–2100) and RCP8.5 (2071–2100) scenarios, respectively. TW_{max} is the maximum daily value averaged over a 6-h window. The background image was obtained from NASA Visible Earth.

significantly reduce the severity of the projected impacts as annual TW_{max} does not breach the 35 °C threshold in any of the locations considered (Fig. 2). T_{max} would not be likely to exceed 55 °C, except at a couple of locations where the current temperature is already severe (Supplementary Fig. 8). Near Jeddah and Mecca, where the rituals of Hajj take place, TW_{max} under this scenario would be only about 2 °C warmer than the current climate.

Although much of the oil produced in this region eventually ends up in the atmosphere and contributes to global climate change, the same oil brings significant financial benefits to the region. These same benefits enhance the capacity of the region to adapt to climate change. Electricity demands for air conditioner use, for example, would considerably increase in the future to adapt to projected changes in climate and population[23]. Although it may be feasible to adapt indoor activities in the rich oil countries of the region, even the most basic outdoor activities are likely to be severely impacted[12]. In contrast, the relatively poor countries of Southwest Asia with limited financial resources and declining or non-existent oil production will probably suffer both indoors and outdoors. For example, TW_{max} in the coastal region of Yemen in the area around Al-Hudaydah and Aden is projected to reach about 33 °C in extreme years. Under such conditions, climate change would possibly lead to premature death of the weakest—namely children and elderly[1]. A plausible analogy of future climate for many locations in Southwest Asia is the current climate of the desert of Northern Afar on the African side of the

Red Sea, a region with no permanent human settlements owing to its extreme climate.

References

1. Sherwood, S. C. & Huber, M. An adaptability limit to climate change due to heat stress. *Proc. Natl Acad. Sci. USA* **107**, 9552–9555 (2010).
2. Boden, T. A., Marland, G. & Andres, R. J. (eds) *Global, Regional, and National Fossil-Fuel CO₂ Emissions* (Oak Ridge National Laboratory, US Department of Energy, 2013).
3. IPCC *Climate Change 2013: The Physical Science Basis* (eds Stocker, T. F. *et al.*) (Cambridge Univ. Press, 2013).
4. Hewitson, B. C. *et al.* in *Climate Change 2014: Impacts, Adaptation, and Vulnerability* (eds Barros, V. R. *et al.*) Ch. 21 (IPCC, Cambridge Univ. Press, 2014).
5. Bindoff, N. L. *et al.* in *Climate Change 2013: The Physical Science Basis* (eds Stocker, T. F. *et al.*) Ch. 10, 867–952 (IPCC, Cambridge Univ. Press, 2013).
6. Marcella, M. P. & Eltahir, E. A. B. Effects of mineral aerosols on the summertime climate of southwest Asia: Incorporating subgrid variability in a dust emission scheme. *J. Geophys. Res.* **115**, D18203 (2010).
7. Marcella, M. P. & Eltahir, E. A. B. Modeling the hydroclimatology of Kuwait: The role of subcloud evaporation in semiarid climates. *J. Clim.* **21**, 2976–2989 (2008).
8. Marcella, M. P. & Eltahir, E. A. B. The hydroclimatology of Kuwait: Explaining the variability of rainfall at seasonal and interannual time scales. *J. Hydrometeorol.* **9**, 1095–1105 (2008).

3
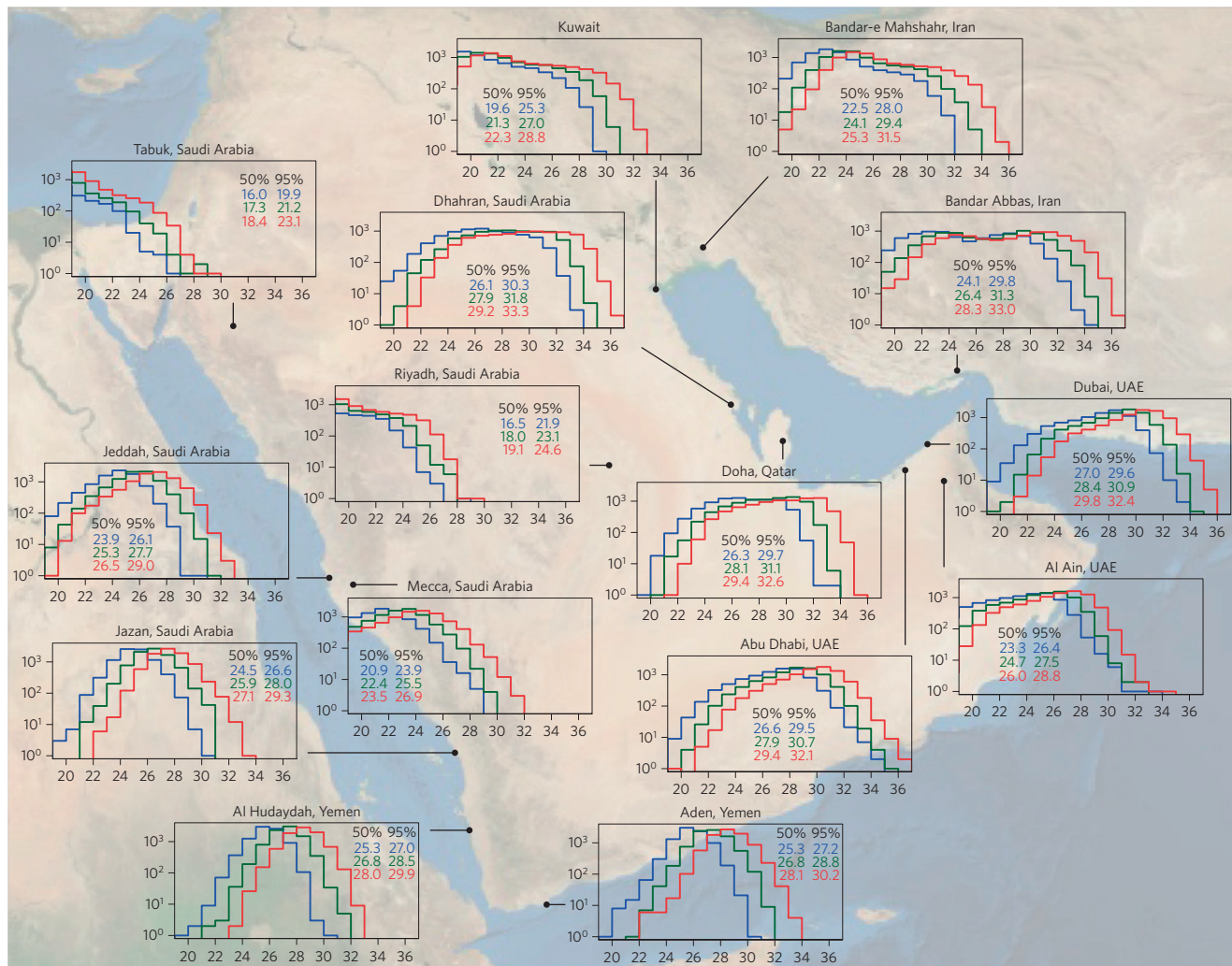
Figure 3 | Histogram of the summer (JAS) TW_{max} for each GHG scenario's ensemble; historical (blue), RCP4.5 (green) and RCP8.5 (red). The histogram bin interval is 0.5 °C and the values on the y-axis indicate the number of exceedances. Values indicated within each plot represent the 50th and 95th percentile event thresholds. TW_{max} is the maximum daily value averaged over a 6-h window. The background image was obtained from NASA Visible Earth.

9. Marcella, M. P. & Eltahir, E. A. B. Modeling the summertime climate of Southwest Asia: The role of land surface processes in shaping the climate of semiarid regions. *J. Clim.* **25**, 704–719 (2011).
10. Rogers, R. R. & Yau, M. K. *A Short Course in Cloud Physics* (Pergamon, 1989).
11. Diffenbaugh, N. S., Pal, J. S., Giorgi, F. & Gao, X. Heat stress intensification in the Mediterranean climate change hotspot. *Geophys. Res. Lett.* **34**, L11706 (2007).
12. Dunne, J. P., Stouffer, R. J. & John, J. G. Reductions in labour capacity from heat stress under climate warming. *Nature Clim. Change* **3**, 563–566 (2013).
13. Fischer, E. M. & Schar, C. Consistent geographical patterns of changes in high-impact European heatwaves. *Nature Geosci.* **3**, 398–403 (2010).
14. Luber, G. & McGeehin, M. Climate change and extreme heat events. *Am. J. Prev. Med.* **35**, 429–435 (2008).
15. Parsons, K. Heat stress standard ISO 7243 and its global application. *Ind. Health* **44**, 368379 (2006).
16. El Fadli, K. I. *et al*. World Meteorological Organization assessment of the purported world record 58 °C temperature extreme at El Azizia, Libya (13 September 1922). *Bull. Am. Meteorol. Soc.* **94**, 199–204 (2013).
17. Cerveny, R. S., Lawrimore, J., Edwards, R. & Landsea, C. Extreme weather records. *Bull. Am. Meteorol. Soc.* **88**, 853–860 (2007).
18. Meinshausen, M. *et al*. The RCP greenhouse gas concentrations and their extensions from 1765 to 2300. *Climatic Change* **109**, 213–241 (2011).
19. Rodwell, M. J. & Hoskins, B. J. Monsoons and the dynamics of deserts. *Q. J. R. Meteorol. Soc.* **122**, 1385–1404 (1996).
20. Thomson, A. *et al*. RCP4.5: A pathway for stabilization of radiative forcing by 2100. *Climatic Change* **109**, 77–94 (2011).
21. Riahi, K. *et al*. RCP 8.5—A scenario of comparatively high greenhouse gas emissions. *Climatic Change* **109**, 33–57 (2011).
22. *World Population Prospects: The 2012 Revision, Methodology of the United Nations Population Estimates and Projections* Working Paper No. ESA/P/WP.235 (United Nations, Department of Economic and Social Affairs, Population Division, 2014).
23. Sailor, D. Air conditioning market saturation and long-term response of residential cooling energy demand to climate change. *Energy* **28**, 941–951 (2003).

Acknowledgements

Author contributions
E.A.B.E. conceived the study with input from J.S.P. Both authors were involved in design of the research, interpretation of the results, and discussion of implications. J.S.P. performed the simulations, analysed the data and created the figures. Both authors contributed equally to the writing and revision of the manuscript.

Additional information
Supplementary information is available in the online version of the paper. Reprints and permissions information is available online at www.nature.com/reprints. Correspondence and requests for materials should be addressed to E.A.B.E.

Competing financial interests
The authors declare no competing financial interests.